

Organic & Biomolecular Chemistry

Accepted Manuscript



This is an *Accepted Manuscript*, which has been through the Royal Society of Chemistry peer review process and has been accepted for publication.

Accepted Manuscripts are published online shortly after acceptance, before technical editing, formatting and proof reading. Using this free service, authors can make their results available to the community, in citable form, before we publish the edited article. We will replace this *Accepted Manuscript* with the edited and formatted *Advance Article* as soon as it is available.

You can find more information about *Accepted Manuscripts* in the [Information for Authors](#).

Please note that technical editing may introduce minor changes to the text and/or graphics, which may alter content. The journal's standard [Terms & Conditions](#) and the [Ethical guidelines](#) still apply. In no event shall the Royal Society of Chemistry be held responsible for any errors or omissions in this *Accepted Manuscript* or any consequences arising from the use of any information it contains.

Planar-Rotor Architecture Based Pyrene-Vinyl-Tetraphenylethylene Conjugated Systems: Photophysical Properties and Aggregation Behavior

Debabrata Jana,^a Shatabdi Boxi,^a Partha P. Parui,^b and Binay K. Ghorai*^a

^a*Department of Chemistry, Indian Institute of Engineering Science and Technology, Shibpur, Howrah 711 103, India*

^b*Department of Chemistry, Jadavpur University, Kolkata 700 032, India*

Tel: +91-33-26684561; Fax: +91-33-26682916; E.mail: binay@chem.iests.ac.in

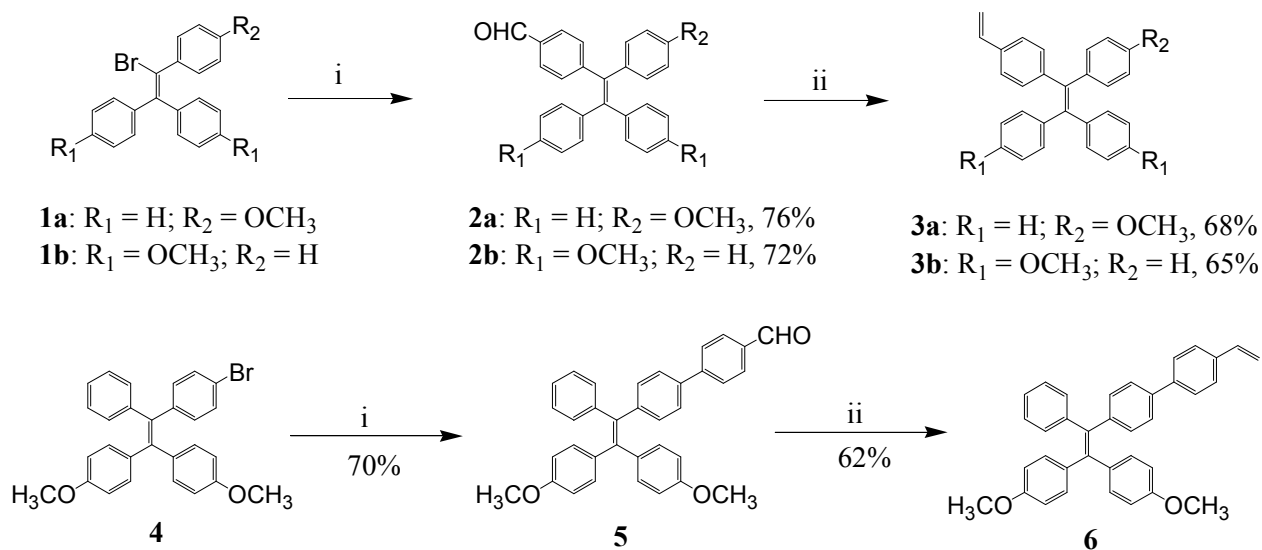
Abstract

Four pyrene-vinyl-tetraphenylethylene based conjugated materials were synthesized and characterized by FT-IR, NMR, and mass spectroscopy. The photophysical (including absorption, fluorescence, and fluorescence lifetime) and aggregation properties in tetrahydrofuran were investigated. The photophysical and aggregation behavior depends on spacer, substituent, and also the architecture (mono or tetra-branched) of the molecule. Vinyl spacer mono-branched compound is aggregation induced emission (AIE) active ($\alpha_{\text{AIE}} = \sim 6$). Vinyl spacer tetra-branched compounds are AIE inactive, but their emitting efficiency is good in both solution ($\Phi_{\text{fl}} = 63\%$) phase and in the aggregated state ($\Phi_{\text{fl}} = 43\%$). Phenylvinyl spacer tetra-branched compounds emit light strongly in solution ($\Phi_{\text{fl}} = 92\%$), but not in the aggregated state ($\Phi_{\text{fl}} = 8\%$). They are shown to be thermally stable and emit light in the green region (500–550 nm). The results of cyclic voltammetry measurements of these materials showed irreversible oxidation wave, and have high HOMO energy level (–5.66 to –5.53 eV).

Introduction

Pyrene (Py) and its derivatives have been extensively studied as emitting materials in optoelectronic applications due to their excellent photophysical properties such as high fluorescence quantum efficiency in dilute solution, long fluorescence lifetime, high charge carrier mobility, thermal, and chemical stability.¹ However, the planer structure of pyrene has restricted its use for development of electroluminescence (EL) materials due to the tendency towards π - π stacking and excimer formation in concentrated solution or in the solid state.² Recently, a large number of solid state emitting materials have been reported in the literature.³ Their architecture are mainly based on rotor system. The rotor nature of molecules inhibits the π - π stacking interaction in concentrated solution or in the solid state. One of the most common rotor chromophores is tetraphenylethylene (TPE). It is non-emissive in dilute solution, as its active intramolecular rotations effectively dissipate the energy of the excitons through nonradiative pathways. But, it emits intensely in the aggregated state or in the solid state due to the physical restriction of its intramolecular rotations.⁴ The unique fluorescence behavior of TPE has been utilized for the development of solid-state lighting materials,⁵ biological sensors,⁶ chem-sensors,⁷ explosive detection,⁸ latent finger print⁹ and luminescent polymers.¹⁰ Pyrene and TPE moieties have shown totally different fluorescent properties in solution and in the aggregated state. If these two moieties are combined in a single molecule, it may offer an interesting combination of the photophysical properties and perhaps, a route to new fluorescent materials which emit light both in solution and the aggregated state or solid state. Our strategy is to develop the organic chromophore which emits light in both solution and in the aggregated state or solid state. The routes lead to the attachment of TPE moiety at the 1- or 1-, 3-, 6-, 8-positions of the pyrene ring to affect both the overall photophysical properties and the aggregation behavior. Tang et al.¹¹ developed pyrene-tetraphenylethylene based solid state emitter utilizing four-fold Suzuki coupling in which four tetraphenylethylene units are directly connected to the central pyrene moiety. Introduction of tetraphenylethylene moiety to the pyrene core solve the aggregation caused quenching (ACQ) problem arising from the rigid planar architecture of pyrene moiety. Inspired by this work, we have synthesized pyrene-vinyl-tetraphenylethylene based conjugated materials through conventional Heck coupling. The planar structure of pyrene and the rotor nature of tetraphenylethylene could be beneficial for improving the fluorescence quantum efficiency in both solution and in the solid state. We have discussed

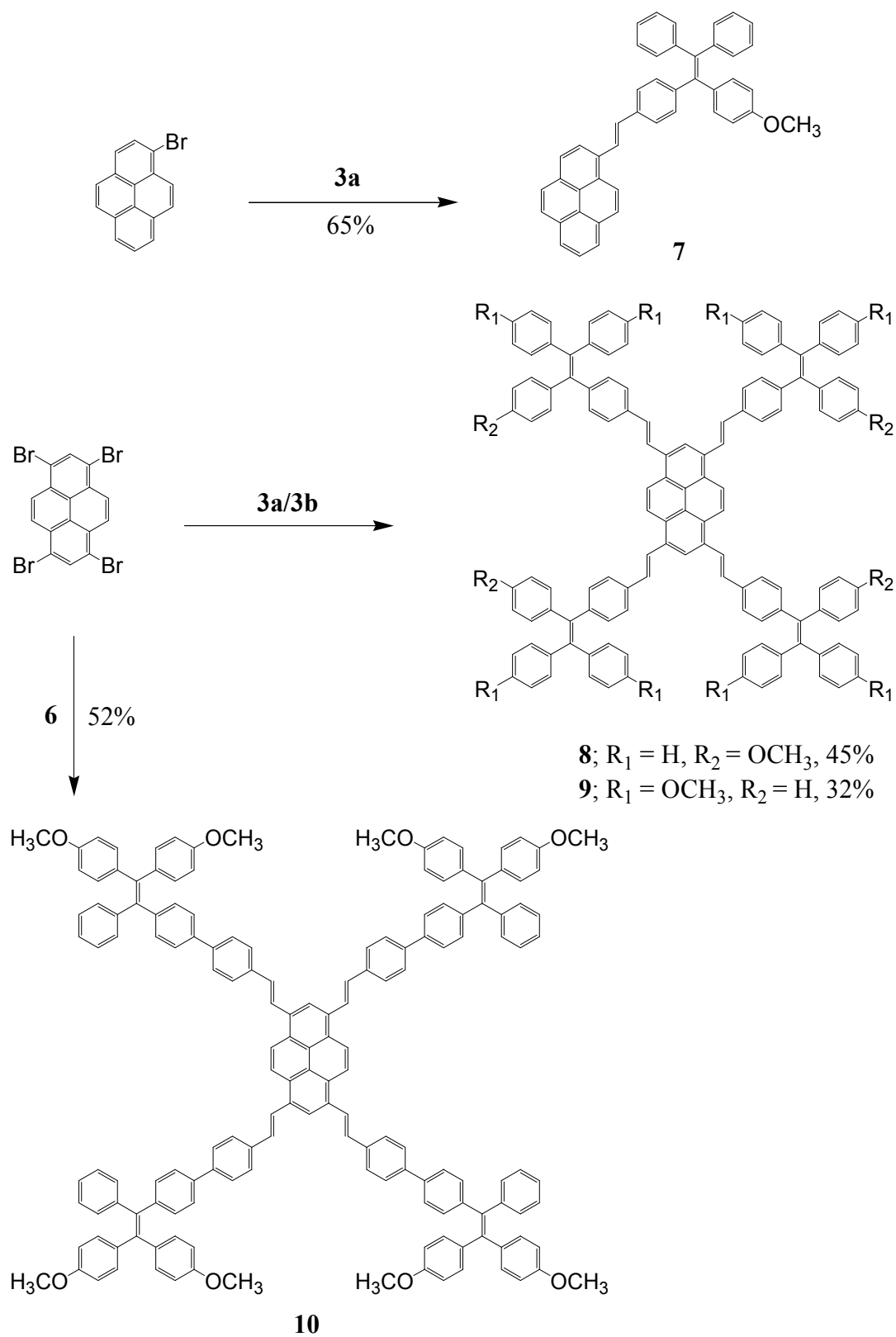
the structures, electrochemical and emitting efficiency in both solution and aggregated state where two different moieties such as pyrene (liquid state emitter) and TPE (solid/aggregate state emitter) are connected through vinyl bond in a mono or tetra-substituted fashion.



Scheme 1 Synthesis of tetraphenylethylene vinyl derivatives **3a–b/6**: *Reagents and conditions:* (i) 4-Formylphenylboronic acid, Pd(PPh₃)₄, K₂CO₃, toluene, H₂O, Aliquat[®] 336, 90 °C, 12 h; (ii) CH₃PPh₃⁺Br⁻, *n*-BuLi, THF, -20 °C, 6 h.

Results and discussion

Our strategy for the synthesis of pyrene-vinyl-tetraphenylethylene derivatives (**7–10**) is based upon conventional palladium catalyzed Heck coupling reaction between the bromo pyrene and vinyl tetraphenylethylene derivatives (**3a/3b/6**). The precursors 1-(1-bromo-2,2-diphenylvinyl)-4-methoxybenzene (**1a**), 1,3,6,8-tetrabromopyrene and compound **1b** were prepared according to the literature procedures.¹² The required vinyl tetraphenylethylene derivatives (**3a/3b/6**) were prepared in two steps, as illustrated in Scheme 1. Suzuki coupling of bromo derivatives (**1a/1b/4**) with 4-formylphenylboronic acid in the presence of a catalytic amount of Pd(PPh₃)₄ followed by Wittig reaction with methyl triphenylphosphonium bromide and *n*-BuLi at -20 °C in tetrahydrofuran afforded **3a**, **3b** and **6** in 72%, 75% and 85% yield, respectively. The synthetic route for compounds **7–10** are depicted in Scheme 2. Heck coupling of 1-bromopyrene with 1.5 equivalent **3a** gave compound **7** (65% yield). Treatment of 1,3,6,8-tetrabromopyrene with 4.5



Scheme 2 Synthesis of pyrene-vinyl-tetraphenylethylene derivatives (**7–10**) using Heck reaction: Pd(OAc)₂, P(*o*-tol)₃, DMF, Et₃N, 90 °C, 24–36 h.

equivalent of **3a** under similar condition afforded **8** in 32% yield. Compounds **9** and **10** were prepared in 45% and 52% yield respectively using same procedure as described for compound **8**. The structures of the final compounds were confirmed by ^1H & ^{13}C NMR spectroscopy, and MALDI-TOF MS/ HRMS measurement. In the ^1H NMR spectra, appearance of the peak at δ 8.45–7.99 confirmed the presence of pyrene moiety. Particularly, for the vinyl moiety we don't get any *trans*-coupled ($-\text{CH}=\text{CH}-$) peak in ^1H NMR spectra, which may be due to overlapping with the excess proton peaks in the aromatic region. But in ^{13}C NMR spectrum, peak at δ 112.6 (for **7**), 113.0 (for **9**) and 113.0 (for **10**) confirmed the presence of vinyl moiety. The presence of methoxy group in the final compound was confirmed by NMR spectra. The singlet at δ 3.76 (for **7**), 3.76 (for **8**), 3.76 (for **9**) and 3.76 (for **10**) in the ^1H NMR spectra and peak at δ 54.6 (for **7**), 55.1 (for **9/10**) in the ^{13}C NMR spectra indicated the presence of methoxy group. The methoxy group present in final compound facilitates the solubility in the common organic solvents such as toluene, dichloromethane and tetrahydrofuran. Finally in the MALDI-TOF MS spectra, dominant peak at m/z 1749.1148 (100%) for **8**, m/z 1869.3167 (100%) for **9** and m/z 2173.8633 (100%) for **10** was observed using dithranol as a matrix, corresponding to the molecular ion mass of respective compounds. The HRMS of compound **7** revealed a peak at 627.2069 ($M^+ + K$), due to the metallation of methoxy group with potassium ion.

The molecular structure in the ground state (in vacuum) of the **7–10** optimized by using ab initio HF/6-31G calculations, are shown in Fig. 1. For simplifying calculation methoxy groups are omitted. All molecules have non-coplanar twisted conformation due to the large torsional angle between pyrene and vinyl moieties. It is well known that TPE moiety is non-planar in nature. We are concerned about the planar nature of vinyl moiety with respect to pyrene. From our calculations it has been found those pyrene moiety and vinyl spacers are not co-planar to each other. Distortions of planarity or dihedral angle between pyrene moiety and vinyl spacer are described as α . The calculated α values are 39° ($\text{C}_{12}\text{-C}_{11}\text{-C}_{25}\text{-C}_{27}$) for **7**, 49° ($\text{C}_3\text{-C}_2\text{-C}_{72}\text{-C}_{73}$) for **8/9** and 49° ($\text{C}_3\text{-C}_2\text{-C}_{23}\text{-C}_{24}$) for **10**. Such a unique structural feature prevents the excessive intermolecular interaction against fluorescence quenching in the solid state.

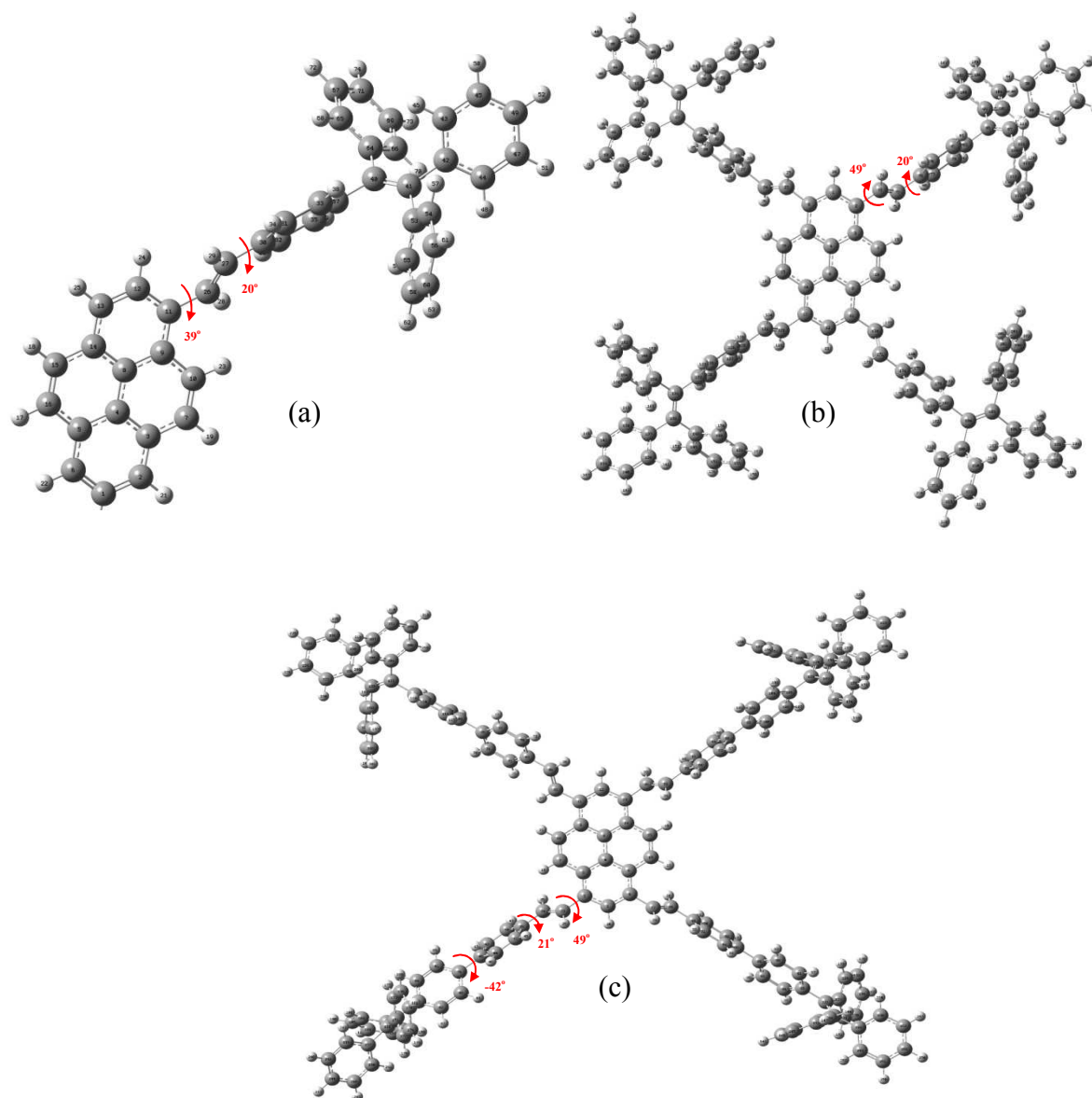


Fig. 1 Optimized structures of (a) **7**, (b) **8** or **9**, and (c) **10** at HF/6-31G level of theory.

Optical properties

Synthesized compounds contain two parts: one planar pyrene moiety having high emitting property in dilute solution, but not in the aggregated state or solid state; and the rotor tetraphenylethylene moiety, which is non-emissive in dilute solution but emits light intensely in the aggregated state. The absorption spectra of **7–10** in dilute tetrahydrofuran solution are shown in Fig. 2; the photophysical properties data are summarized in Table 1. The absorption spectrum

of **7** contains two major bands located at 296 nm and 396 nm, whereas the absorption spectra of **8–10** exhibit broad bands in the range of 299–452 nm as a result of the flexible nature of the molecules. For **7**, the absorption at 296 nm could be attributed to π - π^* transition from tetraphenylethylene¹³ and the other at 396 was due to π - π^* transition from pyrene moiety.¹⁴ Similarly, for **8–10** two absorption bands appeared in the range around 299–328 nm and 378–392 nm which might be due to the π - π^* transition from substituted tetraphenylethylene and pyrene moiety, respectively. The absorption band of **8–10** that emerged at 430–451 nm might be ascribed to the n - π^* transitions from methoxy substituted tetraphenylethylene to the pyrene moiety. It should be noted that the absorption band at low-energy region for **9** (450 nm; $\epsilon = 6.7 \times 10^{-4} \text{ M}^{-1} \text{ cm}^{-1}$) and **10** (451 nm; $\epsilon = 6.8 \times 10^{-4} \text{ M}^{-1} \text{ cm}^{-1}$) slightly red shifted relative to **8** (430 nm; $\epsilon = 5.7 \times 10^{-4} \text{ M}^{-1} \text{ cm}^{-1}$), due to the presence of extra methoxy group, facilitating the n - π^* transitions.

Table 1. Photophysical properties for **7–10**

Compd	$\lambda_{abs}(\text{nm})$ ($\epsilon_{max}, \text{M}^{-1} \text{cm}^{-1} \times 10^4$)	$\lambda_{em}(\text{nm}) \{ \Phi^a(\%) \}$			τ^b (ns)	k_r^c ($\times 10^{-9} \text{s}^{-1}$)	k_{norr}^d ($\times 10^{-9} \text{s}^{-1}$)
		Soln.	Aggr.	Powder			
7	296, 396 (3.8) (5.7)	486	499	520	0.31(0.6)	3.12	2.83
		{12}	{78}		1.61(0.4)	0.62	0.55
8	305, 384, 428 (9.7) (6.9) (5.7)	524	538	584	1.12	0.88	0.59
		{66}	{43}				
9	328, 392, 452 (6.8) (5.7) (6.8)	522	534	585	0.47	2.12	2.30
		{48}	{12}				
10	299, 378, 451 (8.1) (9.5) (6.7)	506	553	590	1.44	0.69	0.06
		{92}	{8}				

^a Fluorescence quantum yields (Φ_f), measured in tetrahydrofuran solution using quinine sulphate solution in 0.1 N H_2SO_4 ($\Phi_f = 0.54$) as a reference, excited at 375 nm.

^b τ is the fluorescence lifetime.

^c K_r is the radiative decay constant.

^d K_{norr} is the non radiative decay constant

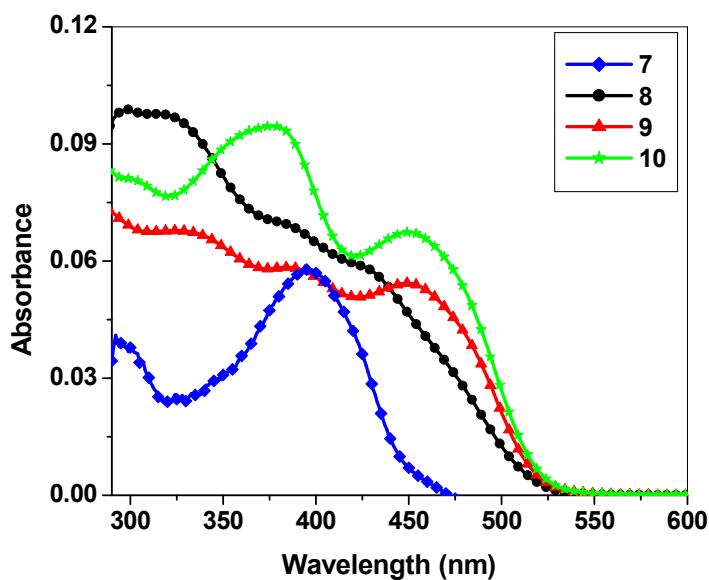


Fig. 2 Absorption spectra of 7–10 in THF ($C = 1 \times 10^{-6}$ M).

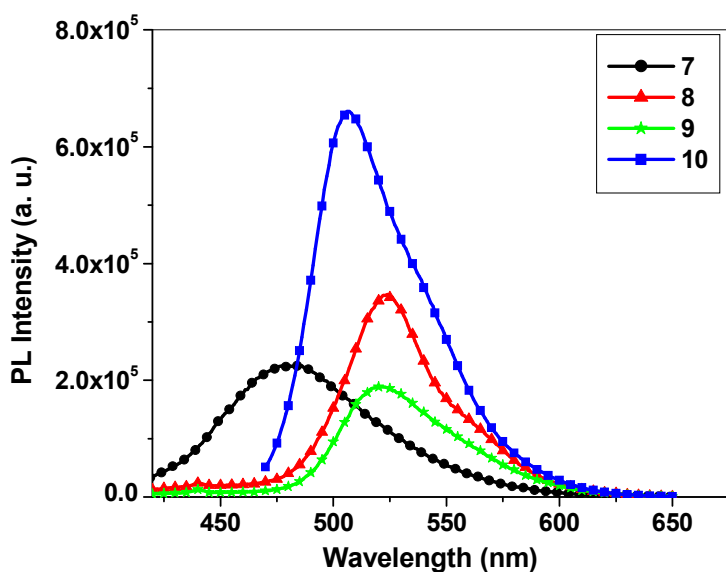


Fig. 3 Emission spectra of 7–10 in THF ($C = 1 \times 10^{-6}$ M).

All compounds 7–10 are fluorescent active. Fig. 3 shows the emission spectra of the 7–10 in dilute THF solution. They display emission peak at 486 nm for 7, 524 nm for 8, 522 nm for 9 and 506 nm for 10, respectively. Clearly, compounds 7 and 8–10 emitted light in blue-green and

green region, respectively in solution. The λ_{em}^{max} value for **8** and **9** is red shifted compared to **7** because tetra-branched structure of **8/9** is having more conjugation possibilities compared to mono-branched structure of **7**. The intense emission at 506 nm of compound **10**, has a marked blue-shift of about 16 nm compared with **9** as a result of reduction of the conjugation, due to the large torsion angle between the central pyrene core and the vinyl-TPE derivative.

The fluorescence quantum yields (Φ_f) of **7–10** in THF were 0.12, 0.66, 0.48 and 0.92 respectively, using quinine sulphate solution in 0.1 N H₂SO₄ ($\Phi_f = 0.54$) as a reference. The Φ_f of **7** is comparative low in THF (0.12). Compound **7** contains one TPE unit and one pyrene unit. The rotor nature of TPE controls the Φ_f value in solution over the planar nature of pyrene. In dilute solution, the unrestricted intramolecular rotation of phenyl rings in TPE moiety can nonradiatively deactivate the excitons and result low Φ_f value. It is interesting to note that the Φ_f value in dilute THF solution of tetra-TPE substituted pyrene (**8/9/10**) is high compared to mono-TPE substituted pyrene (**7**). The planar nature of one pyrene unit controls the Φ_f value in solution over the rotor nature of four TPE. The rigid and twisted structure of **8/9/10** helps to prevent the intermolecular stacking interactions which increase the Φ_f value. Consequently, the Φ_f value of **9** (0.66) decreases compared to **8** (0.48). The basic structural skeleton is same for both **8** and **9**, only the number of methoxy groups present in compound differ. Compounds **8** and **9** contain four and eight methoxy groups, respectively. This behavior is frequently observed in highly polarized molecules exhibiting enlarged dipoles and charge-transfer characters in their excited states, which are referred to as intramolecular charge-transfers (ICT).¹⁵ The charge transfer from methoxy group to the central pyrene moiety in excited state reduces the Φ_f value. But the Φ_f value in dilute solution for compound **10** containing eight methoxy group is relatively high (0.92). The large sterically crowded structure effectively block non-radiative decay pathway of its singlet excited state; making the molecule emissive.¹⁶

Fluorescence transient decays of **7–10** were measured in THF solvent (Fig. 4 and Table 1). Mono-exponential decay profile was observed for **8–10** with a lifetime of 1.12, 0.47 and 1.44 ns respectively, whereas bi-exponential behavior with a lifetime \sim 0.31 and 1.61 ns was identified for compound **7**. This bi-exponential behavior clearly suggests the presence of two emitting species in solutions. One of them is a short one (0.31 ns) with a higher population (60%), whereas the other one has a longer life time (1.61 ns) with a lower population (40%). Rate constants of the radiative (k_r) and non-radiative (k_{nr}) decay of the fluorescence were evaluated

from their respective Φ_f and τ_f values in THF medium. Radiative decay rate constant values (k_r) are $3.12 \times 10^9 \text{ s}^{-1}$, $8.80 \times 10^8 \text{ s}^{-1}$, $2.12 \times 10^9 \text{ s}^{-1}$ and $6.90 \times 10^8 \text{ s}^{-1}$ for compounds **7–10** respectively. The fluorescence lifetime (τ) of the compound is governed by the intra- or inter-molecular interactions present in the molecule. In our synthesized molecule intra- or, intermolecular interaction in Py (such as, π - π stacking, charge transfer etc.) and active intramolecular rotations of phenyl rings in TPE control the fluorescence lifetime. The short fluorescence lifetime of **7** [0.31 ns (60%)] and **9** [0.47 ns] highlighted the presence of intramolecular or intermolecular interactions in the excited state. The τ value is relatively high for **8** (1.12 ns) and **10** (1.44 ns); and also the non-radiative decay rate constant value (k_r) is low for **8** ($5.90 \times 10^8 \text{ s}^{-1}$) and **10** ($5.55 \times 10^7 \text{ s}^{-1}$) relative to **7** and **9**. Following the above fact, it is clear that the presence of intra- or intermolecular interaction in **8/10** is relatively low in the excited state.

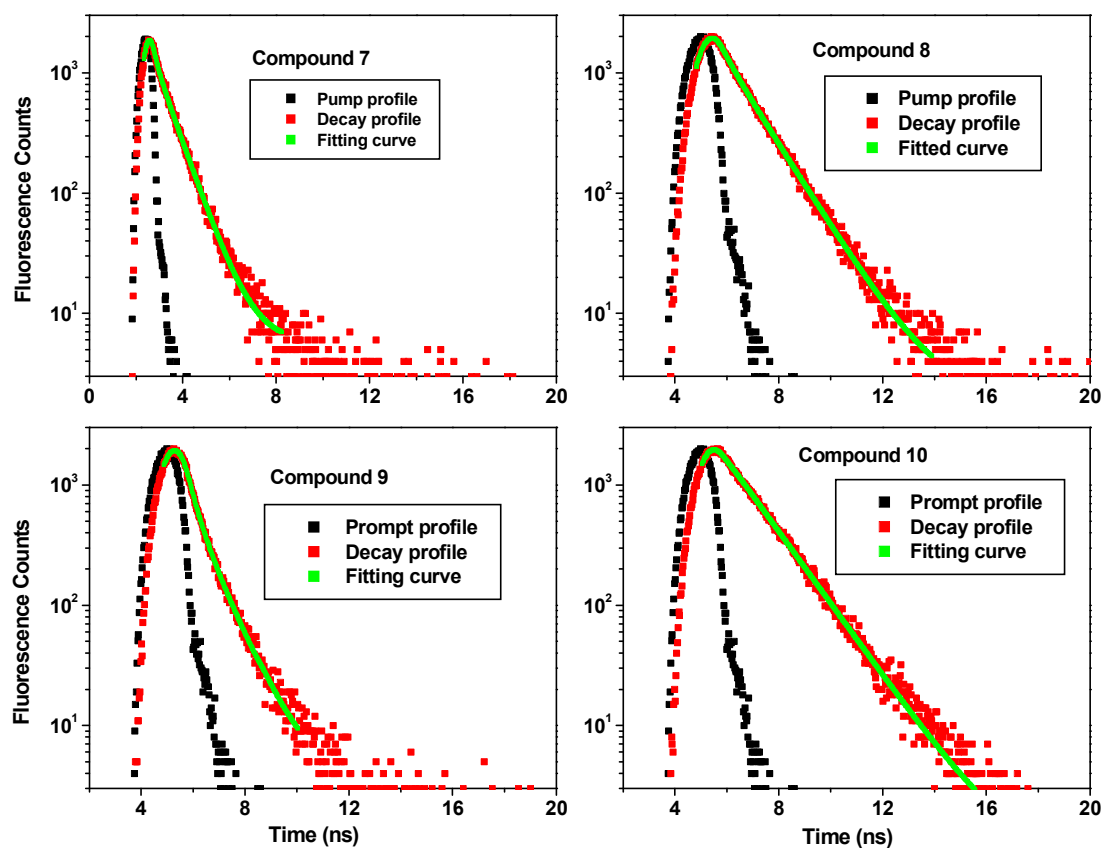


Fig. 4 Fluorescence decay of **7–10** monitored at maximum emission wavelength in THF; excitation wavelength = 370 nm.

Unlike the PL spectrum in solution phase, in the powdered state intense emissions have been observed. Compounds **7–9** are good emitters compared to **10** in powdered state. As expected the planar nature of the pyrene-vinyl-benzene core part quench the emission efficiency in solid state over the rotor nature of tetraphenylethylene part which is known for its solid state emitting property. The emission peaks of compounds **7–10** appeared at 520, 584, 585 and 590 nm, respectively. A slight red shift of the emission maximum of **7–10** can be observed, moving from solution to powdered state. These red-shifted emissions may be induced by the increased planarity and excitonic coupling.¹⁷

Aggregation behavior

To understand the aggregation behavior of **7–10**, their fluorescence study in tetrahydrofuran-water mixtures with different water fractions were carried out. By gradual addition of water (non-solvent) in the THF solution of these fluorophores, the molecular aggregation occurs, which leads to the change in PL intensity. Now variations of the PL peak intensities versus wavelength were studied and depicted in Fig.5. The emission images of these compounds in pure THF and different water fraction mixtures under the 365 nm ultraviolet (UV) illuminations are shown in the inset picture. Gradual addition of water had little effect on the PL spectra of **7** until a mixture of 5:5 water/THF was reached. When the water fraction reached 80%, the PL intensity of **7** was slightly enhanced and at 90% water fraction again the PL intensity increase was about 15-fold compare to pure THF solution.

Particularly for tetra-TPE substituted compounds **8–10** different phenomenon is observed in the aggregation studies. Up to 50% water fraction, the PL intensity slightly decreases relative to those in pure THF solution. At 80% water fraction, the PL intensity increases and then at 90% water fraction again decreases. The PL intensity enhancement of **7** is attributed to the AIEE effect caused by cross-stacking of propeller-like TPE groups when forming molecular aggregates, in which the suppression of π - π stacking interaction and the restriction of intramolecular rotations lead to enhancement of fluorescence intensity.¹⁸ Similarly PL enhancement was observed to the extent of 1.5 fold for the compound **8**. The results indicate that the compound **7** and **8** are AIE-active molecules. In **7** and **8**, rotor-tetraphenylethylene moiety overcomes the ACQ problem caused by planar pyrene counterpart present in the molecule. Surprisingly, for **9–10** different behavior were observed. The PL intensities of **9** and **10** decreased about 2.25-fold and 3-fold, respectively in this aggregation experiment. Compound **9–10** did not show the AIEE property.

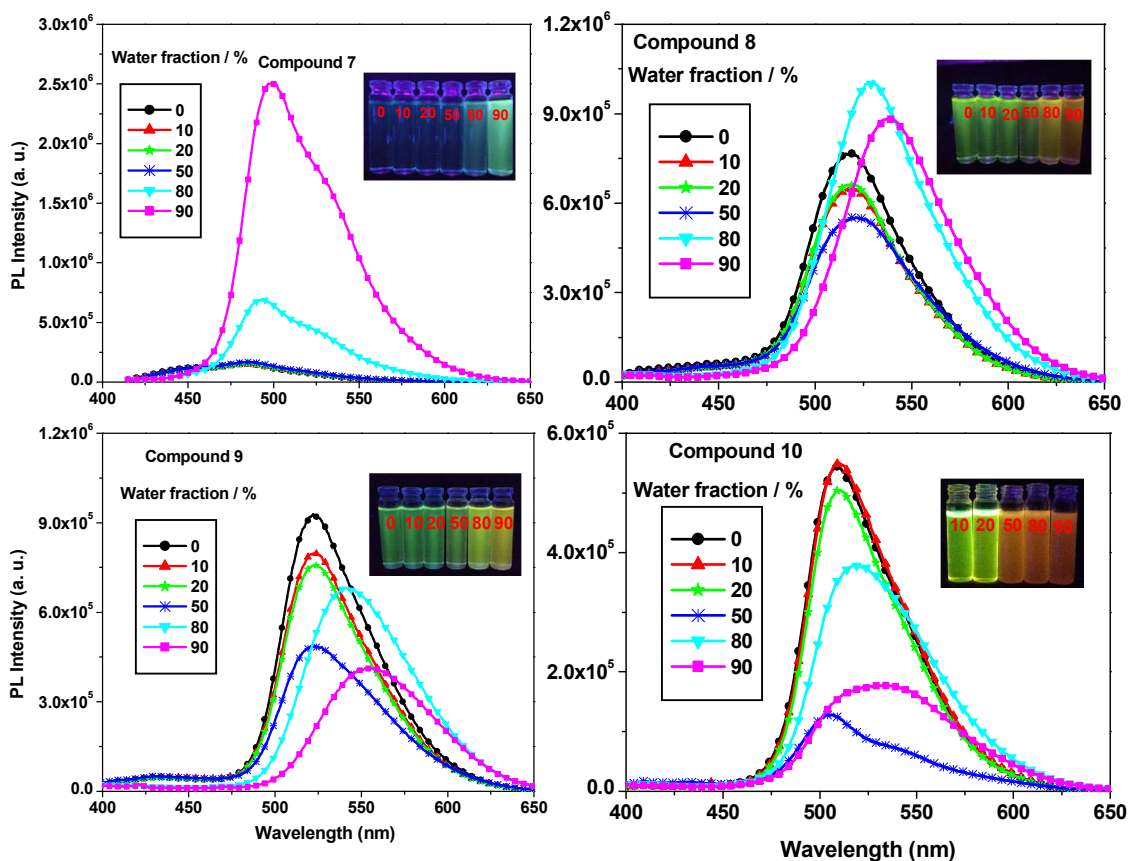


Fig. 5 PL spectra of 7–10 (10 μ M) in THF and with different amounts of water. The inset picture depicts the changes of emission image with water fraction. Excitation wavelength: 392 nm.

In THF solution, compound 7 is less fluorescent than 8–10 but after aggregation the emission enhancement of 7 is relatively more significant than others. To quantitatively estimate the aggregation-induced emission process, the PL quantum yields were calculated for the compounds in the water–THF mixtures with different water fractions. The quantum yield (Φ_f) of 7 was significantly enhanced in solution upon addition of water (Fig. 6). At 90% water fraction, the PL quantum yield of 7 jumped to 78%. The ϕ values of compounds 8–10 at 90% water fraction are 43%, 12% and 8% respectively. Compounds 8–10 contain four TPE units and one pyrene unit; technically they should be AIE active. Surprisingly, the Φ_f value decreases at 90%

water fraction for compound **8–10**. So, ACQ phenomenon dominates over AIE property. This may be due to the presence of four vinyl spacers which push away the rotor counter parts from central planar pyrene moiety and facilitate the ACQ phenomenon. The numbers of methoxy groups present in the compounds have a major influence on the aggregation behavior. For compounds **8** and **9** the Φ_{fl} values at 90% water fraction are 43% and 8% respectively. At 90% water fraction, the Φ_{fl} values decrease due to the increased solvent polarity which facilitates ICT process.¹⁹ The ICT phenomenon depends on the number of methoxy moiety. For **9** and **10** (eight methoxy moieties), ICT is more pronounced than **8** (four methoxy moieties). The large bathochromic shift combined with the decreased Φ_{fl} might be related to the stabilization of the excited state through intramolecular or intermolecular interaction.

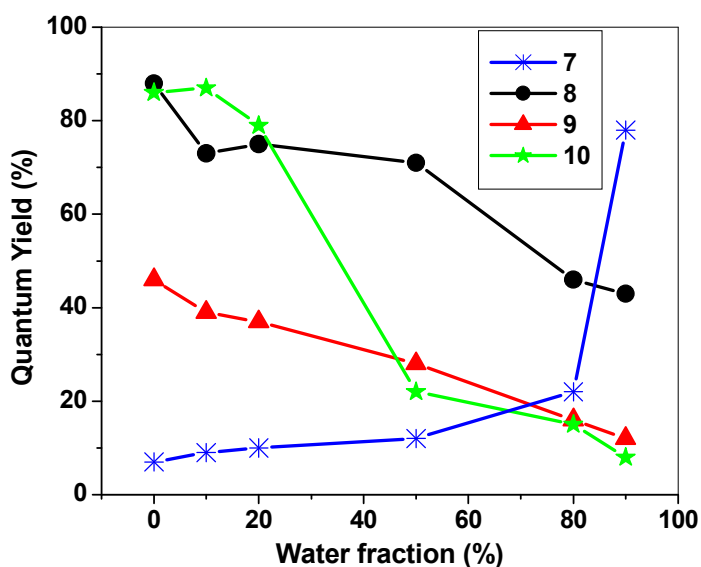


Fig. 6 Plot of quantum yield (%) vs different fraction of water (%) of compounds **7–10**.

The absorption spectra of the compound **7** in water/THF mixture are shown in Fig. 7. The spectral profile was significantly changed when >80% water was added to the THF solution. The entire spectrum showed an increase in absorption, indicating the formation of nanoscopic aggregates of the compounds. The light scattering or Mie effect, of the nanoaggregates suspensions in the solvent mixtures effectively decreased light transmission in the mixture and caused the apparent high absorbance and level-off tail in the visible region of the UV absorption

spectrum.²⁰ With the increasing water content, absorption begins to show gradual red-shifting. The red-shifting of λ_{max} when >80% water is present suggest the formation of J-aggregates.²¹

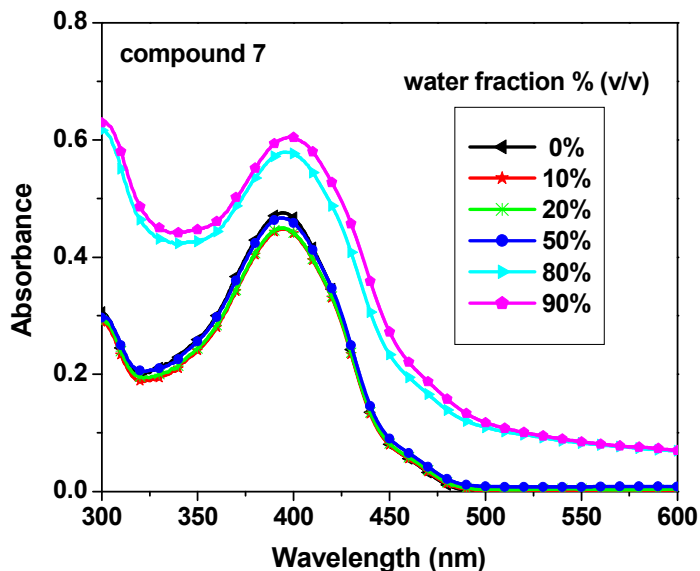


Fig. 7 Absorption spectra of 7 (10 μM) in THF and with different amounts of water.

The thermal properties of 7–10 were analyzed by thermogravimetric analysis (TGA) and are presented in Table 1 and Fig. 8. The thermal decomposition (T_d) temperatures (5% weight loss in nitrogen atmosphere) were observed in the range of 282 to 357 $^{\circ}\text{C}$. These compounds exhibited moderate thermal stabilities. The decomposition temperatures with 5% weight loss under N_2 atmosphere (T_d) for 7, 8, 9 and 10 were 282, 302, 345 and 357 $^{\circ}\text{C}$, respectively. From these T_d values it is clear that the thermal stability depends on the rigid nature of materials in powdered state. More rigid nature induces higher thermal stability particularly for this planar-rotor system. For compound 10, because of its more rigid architecture compared to 7–9, it exhibits good T_d (5%) value. Highly rotor nature compounds 7 and 8 show moderate T_d (5%) value.

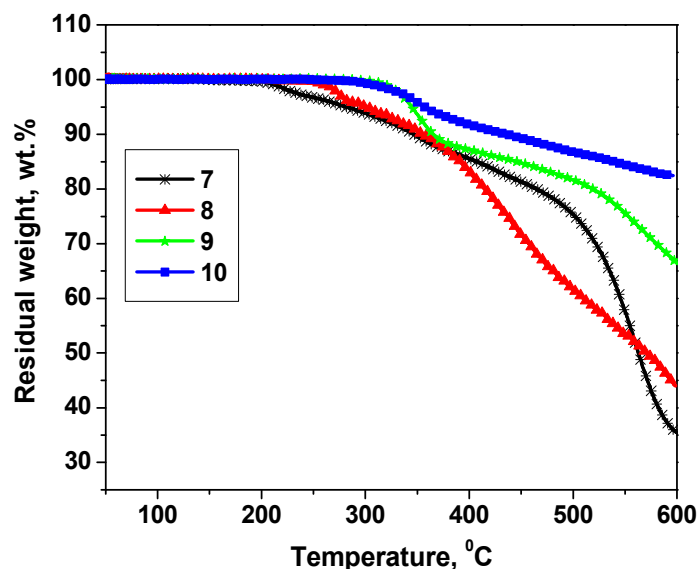


Fig. 8 TGA curves for compounds 7–10 in nitrogen at a heating rate of 10 °C/min

To evaluate the electrochemical behavior of the synthesized oligomer 7–10, cyclic voltammetry measurements were carried out at a scan rate of 100 mV/s in anhydrous dichloromethane using tetrabutylammonium hexafluorophosphate (Bu_4NPF_6 , TBAF) (0.1 M) as an electrolyte and Ag/AgCl as a reference electrode. The cyclic voltammograms of 7–10 are shown in Fig. 9, and the electrochemical properties of all compounds are summarized in Table 2. All compounds 7–10 exhibit irreversible oxidation waves. The onset oxidative potentials for 7–10 were measured as 1.00, 0.94, 0.87 and 0.88 V, respectively. The HOMO levels were calculated by using the known equation $\text{HOMO} = E_{\text{ox}}(\text{onset}) + 4.66 \text{ eV}$.²² Calculating the HOMO-LUMO gap (measured from the absorption maxima), the LUMO levels are found to be ~2.51–2.77 eV. The numbers of electron donating moieties (methoxy group) control the HOMO energy levels. The presence of eight methoxy groups in compounds 9 and 10 exhibited higher HOMO energy levels. The HOMOs of compounds 9 and 10 were estimated to be –5.53 and –5.54 eV, respectively; these values are slightly higher than that of the HOMO of 7 (–5.66 eV) and 8 (–5.60 eV) which contain only one and four methoxy groups, respectively. The HOMO-LUMO gaps (ΔE) of samples 7–10 are 3.15, 2.90, 2.76 and 2.77 eV, respectively. The low value of ΔE for tetra TPE substituted pyrene (8/9/10) can be attributed to the extended π -conjugated system of four vinylene substituted tetraphenylethylene groups. The ΔE values of 9 and 10 are almost

equal; in spite of both compounds having different spacer units. The result clearly demonstrates that the electron donating ability of **9** and **10** are close to each other.

Table 2. Electrochemical properties of compounds **7–10**

Compd	$E_{\text{ox}}(\text{onset})$ (eV)	HOMO/LUMO ^a (eV)	ΔE^b (eV)	T_d^c (°C)
7	1.00	-5.66/-2.51	3.15	282
8	0.94	-5.60/-2.70	2.90	302
9	0.87	-5.53/-2.77	2.76	345
10	0.88	-5.54/-2.77	2.77	357

^a HOMO = $-[E_{\text{ox}}(\text{onset}) + 4.66 \text{ eV}]$; LUMO = HOMO + ΔE

^b ΔE = HOMO–LUMO gap; Estimated from the onset of the absorption spectra: $1240/\lambda_{\text{onset}}$.

^c Decomposition temperature (T_d , 5% weight loss) obtained from thermogravimetric analysis (TGA).

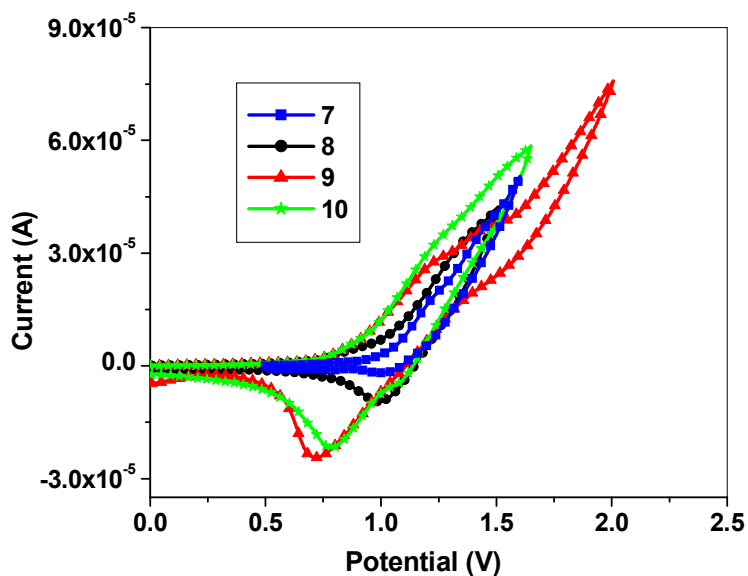


Fig. 9 Cyclic voltammograms of **7–10** ($C = 1 \times 10^{-3} \text{ M}$) in $0.1 \text{ M Bu}_4\text{NPF}_6\text{-CH}_2\text{Cl}_2$, scan rate 100 mV/s .

Conclusions

In summary, four planar-vinyl-rotors configured molecules **7–10** employing two different chromophoric units, such as, pyrene and tetraphenylethylene linked via vinyl/phenylvinyl bond were synthesized for the first time and their photophysical properties and aggregation behavior were studied. The photophysical properties (UV-vis, fluorescence quantum yields and lifetimes) were investigated in THF solution. The molar absorptivity (ϵ) for tetra-substituted compounds is high compare to mono-substituted one. The photophysical and aggregation behavior of **7–10** are dependent on the structure, spacer and also number of methoxy groups. Compound **7** (one pyrene and one TPE unit connected through vinyl bond) showed low Φ_{fl} value in dilute solution (12%) compared to aggregated solution (76%). For compounds **8** and **9** (four TPE units connected to one pyrene unit through vinyl bond) they exhibited good Φ_{fl} value in both solution and aggregated state. However, the Φ_{fl} value in aggregated state for compound **8** (containing four methoxy groups) and **9** (containing eight methoxy groups) is slightly lower than the solution state. Compound **10** (four phenyl-TPE units connected to one pyrene unit through vinyl bond) displayed high Φ_{fl} value in solution (92%) compared to aggregated state (8%). A slight red shift of the emission maximum of **7–10** can be observed from solution to powdered state. The electron donating ability (HOMO energy level) of these compounds depends on the number of methoxy groups present. The HOMOs of compounds **9** and **10** (contains eight methoxy groups) were estimated to be -5.53 and -5.54 eV, respectively; these values are slightly higher than the HOMO of **7** (-5.66 eV) and **8** (-5.60 eV) contains only one and four methoxy groups, respectively. All the compounds enjoy good thermal stability. Further studies addressing the electroluminescence of these compounds are under investigation in our laboratory.

Experimental

General information

All melting points are uncorrected. Unless otherwise noted, all reactions were carried out under an inert atmosphere in flame dried flasks. Solvents obtained from Spectrochem were dried and purified by distillation before use as follows: tetrahydrofuran and toluene from sodium benzophenone ketyl; dichloromethane from P_2O_5 ; DMF from CaH_2 ; triethylamine from solid KOH. After drying, organic extracts were evaporated under reduced pressure and the residue was column chromatographed on silica gel (Spectrochem, particle size 100–200 mesh), using an ethyl

acetate–petroleum ether (60–80 °C) mixture as eluent unless specified otherwise. 4-formylphenylboronic acid, methyltriphenylphosphine bromide, tri(*o*-tolyl)phosphine, *n*-BuLi (1.6 M), Pd(PPh₃)₄ Pd(OAc)₂ were purchased from Aldrich and used as received. 1-(1-Bromo-2,2-diphenylvinyl)-4-methoxybenzene (**1a**), compound **1b** and **4** were synthesized according to the literature procedure.¹²

General procedure for preparation of TPE aldehyde derivatives (**2a–b/5**)

To a solution of **1a–b/4** (2.50 mmol) and 4-formylphenylboronic acid (450 mg, 3.0 mmol) in toluene (12 mL) was added tricaprylylmethylammoniumchloride (Aliquat[®] 336) (3 drops) and 2M potassium carbonate aqueous solution (3 mL). The mixture was stirred for 0.5 h under argon atmosphere. Pd(PPh₃)₄ (10 mg) was added to the reaction mixture and stirred at 90 °C for 12 h. After cooling to room temperature, reaction mixture was poured into water (15 mL) and extracted with ethyl acetate (3×10 mL). The organic layer was dried over anhydrous Na₂SO₄. Solvent was removed under reduced pressure and the residue was purified using column chromatography (silica gel/ethyl acetate: petroleum ether 5:95) afforded the desired compounds **2a–b/4**.

Compound 2a. Light yellow solid; M.P: 82–85 °C; IR (KBr, cm⁻¹): 3012, 2964, 1695, 1596; ¹H NMR (400 MHz, CDCl₃): δ 9.90 (s, 1H), 7.62 (d, 2H, *J* = 8.0 Hz), 7.21 (d, 2H, *J* = 8.0 Hz), 7.18–6.99 (m, 10H), 6.92 (d, 2H, *J* = 8.4 Hz), 6.67 (d, 2H, *J* = 8.4 Hz), 3.74 (s, 3H); ¹³C NMR (100 MHz, CDCl₃): δ 191.9, 158.5, 150.9, 143.4, 143.3, 142.2, 139.4, 135.3, 134.3, 132.5, 132.0, 131.4, 131.3, 129.2, 128.0, 127.9, 126.9, 126.8, 113.4, 55.2; HRMS (ESI): *m/z* calcd for C₂₈H₂₂NaO₂ (M⁺+Na): 413.1517. Found: 413.1516.

Compound 2b. Yellow solid; M.P: 104–105 °C; IR (KBr, cm⁻¹): 3031, 2956, 2835, 1695, 1600; ¹H NMR (500 MHz, CDCl₃): δ 9.90 (s, 1H), 7.61 (d, 2H, *J* = 7.5 Hz), 7.18 (d, 2H, *J* = 7.5 Hz), 7.16–7.09 (m, 3H), 7.08–6.99 (m, 2H), 6.92 (d, 4H, *J* = 8.5 Hz), 6.66 (d, 4H, *J* = 8.5 Hz), 3.74 (s, 6H); ¹³C NMR (125 MHz, CDCl₃): δ 192.0, 158.7, 158.6, 158.5, 151.4, 143.6, 142.4, 138.1, 135.77, 135.72, 134.1, 132.8, 132.7, 132.1, 131.4, 129.3, 128.1, 126.6, 113.3, 113.2, 55.2; HRMS (ESI): *m/z* calcd for C₂₉H₂₄O₃ (M⁺): 420.1725. Found: 420.1722.

Compound 5. Yellow solid, M.P: 112–113 °C; IR (KBr, cm^{-1}): 3027, 2956, 2930, 1698, 1604; ^1H NMR (400 MHz, CDCl_3): δ 10.01 (s, 1H), 7.89 (d, 2H, $J = 8.4$ Hz), 7.70 (d, 2H, $J = 8.4$ Hz), 7.39 (d, 2H, $J = 8.4$ Hz), 7.16–7.02 (m, 7H), 6.99 (d, 2H, $J = 8.4$ Hz), 6.95 (d, 2H, $J = 8.4$ Hz), 6.65 (t, 4H, $J = 8.7$ Hz), 3.73 (s, 6H); ^{13}C NMR (100 MHz, CDCl_3): δ 192.0, 158.3, 158.2, 146.8, 144.9, 144.1, 140.9, 138.5, 136.9, 136.2, 135.0, 132.73, 132.7, 132.1, 131.5, 130.0, 127.9, 127.4, 126.6, 126.3, 113.2, 113.1, 55.1; HRMS (ESI): m/z calcd for $\text{C}_{35}\text{H}_{28}\text{O}_3\text{Na}$ ($\text{M}^+ + \text{Na}$): 519.1936. Found: 519.1934.

General procedure for preparation of vinyl TPE derivatives (3a–b/6)

To a stirred solution of methyl triphenylphosphonium bromide (3.9 g, 10.9 mmol) in THF (20 mL) was added *n*-BuLi (1.6M in hexane) (6 mL, 9.6 mmol) at -20 °C. The reaction mixture was stirred for 0.5 h at this temperature. A solution of tetraphenylethylene aldehyde derivatives (**2a–b/5**) (7.50 mmol) in THF (15 mL) was added dropwise. The reaction mixture was allowed to come to room temperature within 6 h. The mixture was quenched with saturated aqueous NH_4Cl solution (5 mL). The reaction mixture was extracted with dichloromethane (50 mL) and dried over anhydrous Na_2SO_4 . The solvent was removed and purified by column chromatography on silica gel (petroleum ether) yielded compound **3a–b/6**.

Compound 3a. White solid; M.P: 93–95 °C; IR (KBr, cm^{-1}): 3023, 2944, 2926, 1600; ^1H NMR (300 MHz, CDCl_3): δ 7.14 (d, 2H, $J = 8.4$ Hz), 7.13–6.90 (m, 12H), 6.93 (d, 2H, $J = 8.4$ Hz), 6.63 (d, 2H, $J = 8.4$ Hz), 6.61 (dd, 1H, $J = 17.7, 10.8$ Hz), 5.66 (d, 1H, $J = 17.7$ Hz), 5.17 (d, 1H, $J = 10.8$ Hz), 3.73 (s, 3H); ^{13}C NMR (75 MHz, CDCl_3): δ 158.1(s), 144.0 (s), 139.7 (s), 140.8 (s), 136.6 (d), 136.0 (s), 135.4 (s), 132.6 (d), 131.6 (d), 131.4 (d), 127.7 (d), 126.3 (d), 126.2 (d), 125.5 (d), 113.4 (t), 113.0 (d), 55.1 (q); HRMS (ESI): m/z calcd for $\text{C}_{29}\text{H}_{25}\text{O}$ (MH^+): 389.1905. Found: 389.1900.

Compound 3b. White solid; M.P: 163–165 °C; IR (KBr, cm^{-1}): 3005, 2952, 2930, 1600; ^1H NMR (500 MHz, CDCl_3): δ 7.16 (d, 2H, $J = 8.0$ Hz), 7.14–7.08 (m, 3H), 7.03 (d, 2H, $J = 7.0$ Hz), 6.97 (t, 4H, $J = 8.0$ Hz), 6.94 (d, 2H, $J = 8.0$ Hz), 6.68–6.59 (m, 5H), 5.67 (d, 1H, $J = 17.5$ Hz), 5.18 (d, 1H, $J = 11.0$ Hz), 3.75 (s, 3H), 3.74 (s, 3H); ^{13}C NMR (75 MHz, CDCl_3): δ 158.3, 158.2, 144.3, 144.1, 140.3, 138.9, 136.7, 136.4, 135.2, 132.7, 131.6, 131.5, 127.8, 126.2, 125.7, 113.2, 113.1, 55.2; HRMS (ESI): m/z calcd for $\text{C}_{33}\text{H}_{26}\text{O}_2$ (M^+): 418.1933. Found: 418.1982.

Compound 6. Light yellow solid; M.P: 140–142 °C; IR (KBr, cm^{-1}): 3001, 2952, 2930, 2903, 1604; ^1H NMR (400 MHz, CDCl_3): δ 7.53 (d, 2H, $J = 8.0$ Hz), 7.44 (d, 2H, $J = 8.0$ Hz), 7.37 (d, 2H, $J = 8.0$ Hz), 7.16–7.06 (m, 7H), 7.00 (d, 2H, $J = 8.0$ Hz), 6.96 (d, 2H, $J = 8.0$ Hz), 6.74 (dd, 1H, $J = 17.6, 10.8$ Hz), 6.66 (t, 4H, $J = 7.8$ Hz), 5.77 (d, 1H, $J = 17.6$ Hz), 5.25 (d, 1H, $J = 10.8$ Hz), 3.74 (s, 6H); ^{13}C NMR (100 MHz, CDCl_3): δ 158.2, 158.1, 144.3, 143.5, 140.4, 140.1, 138.8, 138.0, 136.5, 136.4, 132.7, 131.9, 131.5, 127.8, 126.9, 126.6, 126.2, 126.1, 113.8, 113.2, 113.0, 55.1; HRMS (ESI): m/z calcd for $\text{C}_{36}\text{H}_{30}\text{NaO}_2$ ($\text{M}^+ + \text{Na}$): 517.2143. Found: 517.2143.

General procedure for preparation of pyrene-vinyl-tetraphenylethylene based conjugated materials (7–10)

A mixture of 1,3,6,8-tetrabromopyrene (92 mg, 0.672 mmol), tetraphenylethylene vinyl derivatives (**3a–b/6**) (3.02 mmol) and $\text{P}(o\text{-tol})_3$ (5 mg, 1.64 mmol) in dry DMF (6 mL) was stirred for 15 min in a double necked round-bottomed flask in an argon atmosphere at room temperature. To this reaction mixture, triethylamine (3 mL) was added and stirred for 15 min. Catalytic amount of $\text{Pd}(\text{OAc})_2$ (10 mg) was added and heated for 24h at 90 °C. The mixture was cooled to room temperature and poured into water (50 mL). The mixture was extracted with dichloromethane (30 mL). The organic layer was washed with water (3×5 mL), brine (5 mL), and dried over anhydrous Na_2SO_4 . Solvent was removed in a rotary evaporator and the crude product was purified using column chromatography to give the compounds **7–10**.

Compound 7. Light yellow solid; M.P: 113–115 °C; IR (KBr, cm^{-1}): 3015, 2925, 2855, 1601; ^1H NMR (500 MHz, CDCl_3): δ 8.45 (d, 1H, $J = 8.5$ Hz), 8.27 (d, 1H, $J = 8.5$ Hz), 8.20–

8.09 (m, 5H), 8.04 (s, 2H), 7.99 (t, 1H, $J = 7.5$ Hz), 7.43 (d, 2H, $J = 8.0$ Hz), 7.25 (t, 2H, $J = 8.0$ Hz), 7.20–7.08 (m, 12H), 7.00 (d, 2H, $J = 8.0$ Hz), 6.68 (d, 2H, $J = 8.0$ Hz), 3.76 (s, 3H); ^{13}C NMR (100 MHz, CDCl_3): δ 157.7, 143.6, 143.5, 143.3, 139.8, 139.7, 135.5, 135.2, 132.2, 131.4, 131.0, 130.98, 130.9, 130.4, 130.0, 127.8, 127.3, 127.2, 127.0, 126.9, 126.7, 125.9, 125.8, 125.6, 125.5, 124.7, 124.6, 124.58, 124.53, 124.4, 123.0, 122.5, 112.6, 54.6; HRMS (ESI): m/z calcd for $\text{C}_{45}\text{H}_{32}\text{KO} [\text{M}^+ + \text{K}]$: 627.2090. Found: 627.2069.

Compound 8. Orange solid; M.P: 72–75 °C; IR (KBr, cm^{-1}): 3050, 2926, 2855, 1600; ^1H NMR (500 MHz, CDCl_3): δ 8.50–8.05 (m, 10H), 7.80–7.70 (m, 4H), 7.48–7.40 (m, 4H), 7.39–7.29 (m, 4H), 7.22–6.81 (m, 56H), 6.70–6.62 (m, 8H), 3.76 (s, 12H); ^{13}C NMR spectral data was not recorded due to poor solubility; MALDI-TOF MS: m/z calcd for $\text{C}_{132}\text{H}_{99}\text{O}_4 [\text{MH}^+]$: 1749.1961. Found: 1749.1148; Anal. calcd for $\text{C}_{132}\text{H}_{98}\text{O}_4$: C, 90.69; H, 5.65; Found: C, 90.65; H, 5.72.

Compound 9. Brown solid; M.P: 82–85 °C; IR (KBr, cm^{-1}): 3027, 2922, 2847, 1604; ^1H NMR (500 MHz, CDCl_3): δ 8.50–8.00 (m, 10H), 7.50–7.40 (m, 8H), 7.38–7.24 (m, 4H), 7.15–6.90 (m, 44H), 6.68 (d, 8H, $J = 8.5$ Hz), 6.65 (d, 8H, $J = 8.5$ Hz), 3.75 (s, 24H); ^{13}C NMR (100 MHz, CDCl_3): δ 158.2, 158.1, 144.2, 140.4, 139.4, 138.8, 136.3, 135.4, 132.9, 132.8, 132.6, 132.1, 131.9, 131.5, 127.8, 126.2, 125.4, 113.2, 113.0, 55.1; MALDI-TOF MS: m/z calcd for $\text{C}_{136}\text{H}_{107}\text{O}_8 [\text{MH}^+]$: 1869.3000, found 1869.3167; Anal. calcd for $\text{C}_{136}\text{H}_{106}\text{O}_8$: C, 87.43; H, 5.72; Found: C, 87.41; H, 5.78.

Compound 10. Brown solid; M.P: 87–88 °C; IR (KBr, cm^{-1}): 3023, 2952, 2926, 1600; ^1H NMR (500 MHz, CDCl_3): δ 8.60–8.00 (m, 10H), 7.75–7.63 (m, 12H), 7.46–7.30 (m, 12H), 7.20–6.90 (m, 32H), 7.01(d, 8H, $J = 8.4$ Hz), 6.97 (d, 8H, $J = 8.8$ Hz), 6.68 (d, 8H, $J = 8.8$ Hz), 6.65 (d, 8H, $J = 8.8$ Hz), 3.75 (s, 24H); ^{13}C NMR (100 MHz, CDCl_3): δ 158.1, 158.0, 144.3, 143.6,

140.3, 138.8, 137.8, 136.4, 132.6, 131.9, 131.5, 127.8, 127.2, 127.0, 126.2, 126.0, 113.1, 113.0, 55.1; MALDI-TOF MS: m/z calcd for $C_{160}H_{123}O_8$ $[MH^+]$: 2173.6838, Found 2173.6633; Anal. calcd for $C_{160}H_{122}O_8$: C, 88.45; H, 5.66. Found: C, 88.42; H, 5.70.

Acknowledgments

Financial support from CSIR [No. 02(0150)/13/EMR-II], New Delhi is gratefully acknowledged. S.B. is thankful to Indian Institute of Engineering Science and Technology, Shibpur, Howrah for Institute Fellowship.

Reference

- (a) T. M. Figueira-Duarte and K. Müllen, *Chem. Rev.*, 2011, **111**, 7260; (b) J. K. Salunke, P. Sonar, F. L. Wong, V. A. L. Roy, C. S. Lee and P. P. Wadgaonkar, *Phys. Chem. Chem. Phys.*, 2014, **16**, 23320; (c) X. Feng, J.-Y. Hu, H. Tomiyasu, N. Seto, C. Redshaw, M. R. J. Elsegood and T. Yamato, *Org. Biomol. Chem.*, 2013, **11**, 8366; (d) B. Kim, Y. Park, J. Lee, D. Yokoyama, J.-H. Lee, J. Kido and J. Park, *J. Mater. Chem. C*, 2013, **1**, 432; (e) J.-Y. Hu, X.-L. Ni, X. Feng, M. Era, M. R. J. Elsegood, S. J. Teat and T. Yamato, *Org. Biomol. Chem.*, 2012, **10**, 2255; (f) X. H. Yang, T. Giovenzana, B. Feild, G. E. Jabbour and A. Sellinger, *J. Mater. Chem.*, 2012, **22**, 12689; (g) Z.-Q. Liang, Z.-Z. Chu, D.-C. Zou, X.-M. Wang and X.-T. Tao, *Org. Electron.*, 2012, **13**, 2898; (h) J.-F. Gu, G.-H. Xie, L. Zhang, S.-F. Chen, Z.-Q. Lin, Z.-S. Zhang, J.-F. Zhao, L.-H. Xie, C. Tang, Y. Zhao, S.-Y. Liu and W. Huang, *J. Phys. Chem. Lett.*, 2010, **1**, 2849; (i) J.-Y. Hu, M. Era, M. R. J. Elsegood and T. Yamato, *Eur. J. Org. Chem.*, 2010, 72.
- (a) A. T. Haedler, H. Misslitz, C. Buehlmeier, R. Q. Albuquerque, A. Köhler and H.-W. Schmidt, *Chem. Phys. Chem.*, 2013, **14**, 1818; (b) F. Ito, T. Kakiuchi, T. Sakano and T. Nagamura, *Phys. Chem. Chem. Phys.*, 2010, **12**, 10923.

3. (a) H. Li, Y. Guo, G. Li, H. Xiao, Y. Lei, X. Huang, J. Chen, H. Wu, J. Ding and Y. Cheng, *J. Phys. Chem. C*, 2015, **119**, 6737; (b) Y. Ezhumalai, T.-H. Wang and H.-F. Hsu, *Org. Lett.*, 2015, **17**, 536; (c) J. Zhang, B. Xu, J. Chen, L. Wang and W. Tian, *J. Phys. Chem. C*, 2013, **117**, 23117; (d) X. Feng, B. Tong, J. Shen, J. Shi, T. Han, L. Chen, J. Zhi, P. Lu, Y. Ma and Y. Dong, *J. Phys. Chem. B* 2010, **114**, 16731; (e) K. Kokado and Y. Chujo, *J. Org. Chem.*, 2011, **76**, 316; (f) Z. Zheng, Z. Yu, M. Yang, F. Jin, Q. Zhang, H. Zhou, J. Wu and Y. Tian, *J. Org. Chem.*, 2013, **78**, 3222; (g) S. Shin, S. H. Gihm, C. R. Park, S. Kim and S. Y. Park, *Chem. Mater.*, 2013, **25**, 3288.
4. J. Mei, Y. Hong, J. W. Y. Lam, A. Qin, Y. Tang and B. Z. Tang, *Adv. Mater.*, 2014, **26**, 5429.
5. (a) G.-F. Zhang, H. Wang, M. P. Aldred, T. Chen, Z.-Q. Chen, X. Meng and M.-Q. Zhu, *Chem. Mater.*, 2014, **26**, 4433; (b) L. Chen, Y. Jiang, H. Nie, R. Hu, H. S. Kwok, F. Huang, A. Qin, Z. Zhao and B. Z. Tang, *ACS Appl. Mater. Interfaces*, 2014, **6**, 17215; (c) B. Xu, Z. Chi, H. Li, X. Zhang, X. Li, S. Liu, Y. Zhang and J. Xu, *J. Phys. Chem. C*, 2011, **115**, 17574; (d) X. Du, J. Qi, Z. Zhang, D. Ma and Z. Y. Wang, *Chem. Mater.*, 2012, **24**, 2178; (e) J. Li, Y. Duan and Q. Li, *Dyes Pigm.*, 2013, **96**, 391.
6. (a) R. T. K. Kwok, C. W. T. Leung, J. W. Y. Lam, and B. Z. Tang, *Chem. Soc. Rev.*, 2015, **44**, 4228; (b) X. Wang, J. Hu, G. Zhang and S. Liu, *J. Am. Chem. Soc.*, 2014, **136**, 9890; (c) R. Zhang, Y. Yuan, J. Liang, R. T. K. Kwok, Q. Zhu, G. Feng, J. Geng, B. Z. Tang and B. Liu, *ACS Appl. Mater. Interfaces*, 2014, **6**, 14302; (d) C. Zhang, S. Jin, S. Li, X. Xue, J. Liu, Y. Huang, Y. Jiang, W.-Q. Chen, G. Zou and X.-J. Liang, *ACS Appl. Mater. Interfaces*, 2014, **6**, 5212; (e) J. Chen, Y. Wang, W. Li, H. Zhou, Y. Li and C. Yu, *Anal. Chem.*, 2014, **86**, 9866.
7. (a) Y. Liu, C. Deng, L. Tang, A. Qin, R. Hu, J. Z. Sun and B. Z. Tang, *J. Am. Chem. Soc.*, 2011, **133**, 660; (b) F. Sun, G. Zhang, D. Zhang, L. Xue and H. Jiang, *Org. Lett.*, 2011, **13**, 6378;

- (c) X. Huang, X. Gu, G. Zhang and D. Zhang, *Chem. Commun.*, 2012, **48**, 12195; (d) Y. Yan, Z. Che, X. Yu, X. Zhi, J. Wang and H. Xu, *Bioorg. Med. Chem.*, 2013, **21**, 508; (e) C. J. Kassl and F. Christopher Pigge, *Tetrahedron Lett.*, 2014, **55**, 4810.
8. (a) W. Dong, Y. Pan, M. Fritsch and U. Scherf, *J. Polym. Sci. A Polym. Chem.*, 2015, doi: 10.1002/pola.27631; (b) H.-T. Feng and Y.-S. Zheng, *Chemistry*, 2014, **20**, 195.
9. Y. Li, L. Xu and B. Su, *Chem. Commun.*, 2012, **48**, 4109.
10. G. Iasilli, A. Battisti, F. Tantussi, F. Fuso, M. Allegrini, G. Ruggeri and A. Pucci, *Macromol. Chem. Phys.*, 2014, **215**, 499.
11. Z. Zhao, S. Chen, J. W. Y. Lam, P. Lu, Y. Zhong, K. S. Wong, H. S. Kwoka, and B. Z. Tang, *Chem. Commun.*, 2010, **46**, 2221.
12. (a) D. Jana and B. K. Ghorai, *Tetrahedron*, 2012, **68**, 7309; (b) D. Jana and B. K. Ghorai, *Tetrahedron Lett.*, 2012, **53**, 6838.
13. Z. Zhao, J. W. Y. Lam and B. Z. Tang, *J. Mater. Chem.*, 2012, **22**, 23726.
14. (a) R. Muangpaisal, M.-C. Ho, T.-H. Huang, C.-H. Chen, J.-Y. Shen, J.-S. Ni, J. T. Lin, T.-H. Ke, L.-Y. Chen, C.-C. Wue and C. Tsai, *Org. Electron.*, 2014, **15**, 2148; (b) K. L. Chan, J. P. F. Lim, X. Yang, A. Dodabalapur, G. E. Jabbour and A. Sellinger, *Chem. Commun.*, 2012, **48**, 5106; (c) H.-Y. Oh, C. Lee and S. Lee, *Org. Electron.*, 2009, **10**, 163; (d) J. N. Moorthy, P. Natarajan, P. Venkatakrishnan, D.-F. Huang and T. J. Chow, *Org. Lett.*, 2007, **9**, 5215; (e) Y. Sagara, T. Mutai, I. Yoshikawa and K. Araki, *J. Am. Chem. Soc.*, 2007, **129**, 1520.
15. Z. R. Grabowski and K. Rotkiewicz, *Chem. Rev.*, 2003, **103**, 3899.
16. W. Wang, T. Lin, M. Wang, T.-X. Liu, L. Ren, D. Chen and S. Huang, *J. Phys. Chem. B*, 2010, **114**, 5983.

17. X. Zhang, Z. Chi, H. Li, B. Xu, X. Li, W. Zhou, S. Liu, Y. Zhang and J. Xu, *Chem. Asian J.*, 2011, **6**, 808.
18. (a) H. Li, Z. Chi, B. Xu, X. Zhang, Z. Yang, X. Li, S. Liu, Y. Zhang and J. Xu, *J. Mater. Chem.*, 2010, **20**, 6103; (b) S.-B. Han, H.-J. Kim, D. Jung, J. Kim, B.-K. Cho and S. Cho, *J. Phys. Chem. C*, 2015, doi: 10.1021/acs.jpcc.5b03525; (c) H. Liu, J. Xu, Y. Li and Y. Li, *Acc. Chem. Res.*, 2010, **43**, 1496.
19. Y. Li, T. Liu, H. Liu, M.-Z. Tian and Y. Li, *Acc. Chem. Res.*, 2014, **47**, 1186.
20. (a) B. Z. Tang, Y. Geng, J. W. Y. Lam, B. Li, X. Jing, X. Wang, F. Wang, A. B. Pakhomov and X. Zhang, *Chem. Mater.*, 1999, **11**, 1581; (b) M. Lechner, *J. Serb. Chem. Soc.*, 2005, **70**, 361.
20. G. Sun, Y. Zhao and W. Z. Liang, *J. Chem. Theory Comput.*, 2015, **11**, 2257.
21. Z. Yang, B. Xu, J. He, L. Xue, Q. Guo, H. Xia and W. Tian, *Org. Electron.*, 2009, **10**, 954.